ChemComm

COMMUNICATION

View Article Online
View Journal

Cite this: DOI: 10.1039/c7cc00667e

Received 24th January 2017,
Accepted 16th February 2017

DOI: 10.1039/c7cc00667e

rsc.li/chemcomm

Discovery of a new class of highly potent necroptosis inhibitors targeting the mixed lineage kinase domain-like protein†

Bo Yan,‡[ac] Lei Liu,‡[bc] Shaoqiang Huang,[c] Yan Ren,[c] Huayi Wang,[c] Zhenglin Yao,[c] Lin Li,[c] She Chen,[c] Xiaodong Wang*[bc] and Zhiyuan Zhang*[cd]

We report the development of novel Mixed Lineage Kinase Domain-Like protein (MLKL) inhibitors with single nanomolar potency (compound 15 is also named as TC13172). Using the converting biochemistry to chemistry activity-based protein profiling (BTC-ABPP) method, we were able to determine that the inhibitors covalently bind to Cysteine86 (Cys-86) of MLKL. This is the first example of the use of LC-MS/MS to identify the binding site of an MLKL inhibitor. The novel MLKL inhibitors provide powerful tools to study the biological function of MLKL and demonstrate that MLKL should be viewed as a druggable target.

Necroptosis is a type of programmed necrotic cell death involved in organ development, tissue homeostasis, inflammation, and disease pathogenesis.[1] After necroptosis induction, receptor interacting protein kinase 1 (RIP1),[2] RIP3,[3] and MLKL[4] are activated sequentially. MLKL, as the executor of necroptosis, can then form oligomers and translocate to cellular membranes, where it mediates ion influx and/or causes the disruption of cell structures.[5] Recent studies have established that MLKL is involved in multiple human inflammatory diseases, including acute pancreatitis, multiple sclerosis, inflammatory bowel disease, and allergic colitis.[6] In this context, MLKL is viewed as a potential therapeutic target for drug discovery.

There are only two known MLKL inhibitors (Fig. 1): necrosulfonamide (NSA)[4] and GW806742X.[7] The moderate potency and narrow structure–activity relationship (SAR) profile of NSA has limited its development as a drug.[1a,8] GW806742X which targets the pseudo-kinase domain of MLKL has been found to have off-target activity against other kinases, including VEGFR2.[9] Of note, we found in the present study that GW806742X also shows off-target activities against RIP1 and RIP3 (Fig. S1, ESI†), so it is not possible to conclude that the prevention of necroptosis as mediated by GW806742X relies solely on the targeting of MLKL. Given the deficiencies of the MLKL inhibitors reported to date, the development of novel, highly potent MLKL inhibitors will almost certainly benefit research into the role of MLKL in necroptosis-related disease pathogenesis, as well as confirm MLKL as a druggable target.

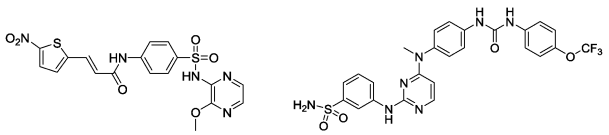

Fig. 1 Chemical structures of previously reported MLKL inhibitors: necrosulfonamide and GW806742X.

In previous work, we performed a cell-based high-throughput screen to identify necroptosis inhibitors using a chemical library of ~200 000 compounds and identified multiple compounds that protected human colorectal adenocarcinoma (HT-29) cells from TNF-α/Smac mimetic/Z-VAD-fmk (TSZ)-induced necroptosis.[4] Among these hits, one was developed into the first MLKL inhibitor NSA which revealed the biological function of MLKL in necroptosis.[4] Another hit was identified as a RIP1 inhibitor and was further developed into the highly potent and selective anti-inflammation reagent RIPA-56.[10] In this work, we investigated another hit from this high-throughput screen, compound **1**, which has good anti-necroptosis potency (EC_{50} = 390 ± 8 nM) (Fig. 2A). We describe how we successfully identified the target of compound **1**, and how, using medicinal chemistry and chemical genetic methods, we developed compound **1** into a series of the most potent MLKL inhibitors ever reported.

In order to determine if compound **1** interacts with an unknown target or interacts with one of the three proteins known to be directly involved in TSZ-induced necroptosis (RIP1, RIP3, and MLKL), we performed several experiments to determine the effect of compound **1** on the functions of RIP1,

[a] School of Life Sciences, Peking University, Beijing, 100871, China
[b] Graduate School of Peking Union Medical College and Chinese Academy of Medical Sciences, Beijing, 100730, China
[c] National Institute of Biological Sciences, Beijing, 102206, China. E-mail: wangxiaodong@nibs.ac.cn, zhangzhiyuan@nibs.ac.cn
[d] Collaborative Innovation Center for Cancer Medicine, Beijing, 102206, China

† Electronic supplementary information (ESI) available. See DOI: 10.1039/c7cc00667e

‡ These authors contributed equally to this work.

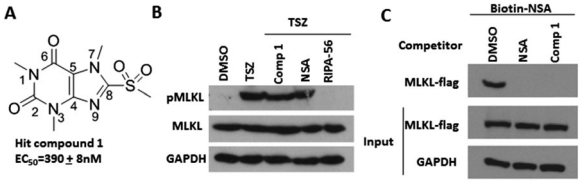

Fig. 2 Compound **1** is a novel inhibitor of necroptosis that may block the function of MLKL. (A) The chemical structure and EC_{50} of compound **1**. EC_{50} determination assays were performed in TSZ-induced HT-29 cells; values were calculated using GraphPad Prism software. (B) Compound **1** does not block the phosphorylation of MLKL. TSZ-treated HT-29 cells were incubated with DMSO, 1 μM compound **1**, 1 μM NSA (known not to inhibit the phosphorylation of MLKL), or 200 nM RIPA-56 (known to inhibit the phosphorylation of MLKL) for 8 h. The samples were analysed by western blotting using antibodies against pMLKL, MLKL and GAPDH. (C) Compound **1** may target MLKL. MLKL-flag-HT-29 cell lysates were pre-incubated with DMSO, or 1 μM compound **1**, or 1 μM NSA (positive control) for 2 h; 10 μM biotin-NSA was then added and incubated for another 2 h. The biotin-NSA-labeled MLKL was precipitated and detected by western blotting using antibodies against flag and GAPDH.

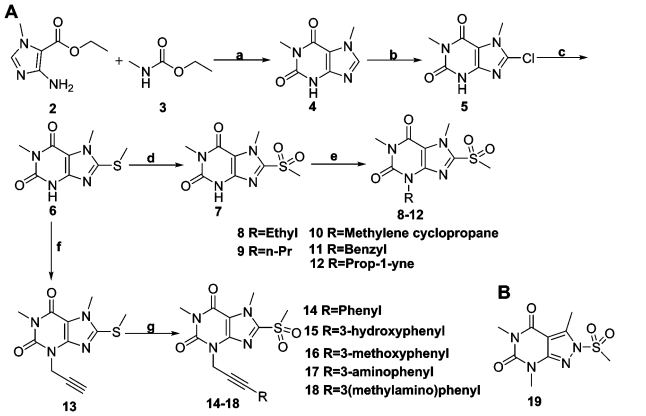

Fig. 3 (A) Synthesis of compounds **7–12** and **14–18**. (a) Potassium *tert*-butanolate, anhydrous THF, 75 °C, overnight; (b) NCS, THF, rt, overnight; (c) NaSMe, DMF, 100 °C, 3 h; (d) oxone, MeOH : H_2O 1 : 1, rt, 4 h; (e) K_2CO_3, DMF, rt, 1 h; (f) 3-bromoprop-1-yne, K_2CO_3, DMF, rt, 1 h; (g) $Pd(PPh_3)_4$, CuI, TEA, anhydrous DMF, 60 °C, 6 h; Oxone, MeOH : H_2O 1 : 1, rt, 4 h. (B) The structure of compound **19**.

RIP3, and MLKL. First, we tested whether compound **1** alters RIP1 and RIP3 kinase activities in enzymatic assays, as their kinase activities are required for the progression of necroptosis (Fig. S2, ESI†). We found that compound **1** did not inhibit the kinase activities of RIP1 or RIP3 at concentrations up to 10 μM, which excluded the possibility of RIPK1 or RIPK3 being the target. Based on western-blot analysis with antibodies against phosphorylated MLKL (pMLKL) (Fig. 2B), compound **1** did not block the phosphorylation of MLKL. However, compound **1** did block the binding of MLKL to NSA according to the binding competition experiment testing the ability of compound **1** to compete with NSA for MLKL binding (Fig. 2C). This suggests that MLKL may be a target of compound **1**.

In order to obtain direct evidence that compound **1** targets MLKL, we employed a chemical genetic method. Specifically, an affinity probe was used to fish out the targets of compound **1**. We synthesized a series of derivatives based on compound **1** with the aim of increasing its anti-necroptosis potency and obtaining a high affinity probe for target identification. We first conducted SAR studies on the 8-/1-/7-position of compound **1** by substituting the original methyl group with various functional groups (Table S1, ESI†). Necroptosis assay results indicated that all of the tested substitutions at the 8-/1-/7-position deleteriously affected potency, revealing that the methyl group is the best of the tested structures at these positions. We then switched our efforts to the 3-position of compound **1**. The related derivative compounds **7–12** and **14–18** were synthesized by the routes showed in Fig. 3A. The imidazole derivative **2** was cyclized with ethyl methylcarbamate (**3**), yielding 1,7-dimethylxanthine (**4**). Subsequent chlorine and mercapto substitution yielded purine derivative **6**, which was oxidized with oxone to yield **7**. The substitution of **7** with different bromo derivatives generated the target compounds **8–12**. Compounds **14–18** were synthesized using intermediate **6** as the starting material. Intermediate **6** was substituted by 3-bromoprop-1-yne, yielding intermediate **13**; subsequent Sonogashira coupling with different iodobenzene derivatives and oxidation with oxone yielded target compounds **14–18**.

Table 1 Potency (EC_{50}) of compounds **7–12** and **14–18** in TSZ-induced necroptosis assays in HT-29 cells

Compound	EC_{50}[a] (nM)	Compound	EC_{50}[a] (nM)
1	390 ± 8	**14**	25 ± 3.4
7	5983 ± 926	**15**	2 ± 0.6
8	2510 ± 130	**16**	35 ± 8.5
9	925 ± 28	**17**	7 ± 1.0
10	651 ± 103	**18**	7 ± 0.2
11	700 ± 21	NSA	447 ± 32
12	152 ± 23	GW806742X	589 ± 12

[a] Necroptosis was induced in HT-29 cells for 24 h; the EC_{50} values given here are the mean values of at least three independent analyses.

The anti-necroptosis potency of compounds **7–12** and **14–18** was evaluated in the HT-29 cell line; the EC_{50} values are shown in Table 1. Lacking the methyl group, compound **7** had a more than 10-fold reduction in potency relative to compound **1**. The ethyl analogue **8** had a 5-fold reduction in potency compared with compound **1**. Further extending the length of the alkyl chain recovered some potency (see compounds **9** and **10**). Interestingly, compound **12**, which has a propyne group, was 3-fold more potent than compound **1** (methyl group); however, the benzyl analogue **11** had a 4-fold reduction in potency relative to compound **12**, suggesting the presence of a relatively narrow hydrophobic space in the target. To probe the putative binding pocket beyond the region defined by the propyne group, we synthesized **14** by adding a phenyl group at the end of the propyne group of **12**. Surprisingly, compound **14** showed a 6-fold improvement in potency over compound **12** suggesting the presence of an 'open space' in this area for generating additional interactions between target and the inhibitors. To look into the possibility of generating an extra hydrogen bond interaction around the phenyl group, we designed and synthesized compounds **15–18**. To our surprise, compounds

15 (**TC13172**; 3-OH), **17** (3-NH_2), and **18** (3-NHMe) had inhibition potency of 2 nM, 7 nM, and 7 nM respectively against cell necroptosis. Conversely, methylation of the 3-OH of compound **15** (compound **16**) resulted in a 15-fold reduction in potency. The potency enhancement with compounds **15**, **17**, and **18** suggested possible hydrogen bond formation between the hydrogen-bond donor, 3-OH of compound **15** (or 3-NHR of compounds **17–18**), and an acceptor residue on the target. The methoxy group of compound **16** (3-OMe) lacks the hydrogen-bond donating property, which abolished hydrogen bond formation and led to the loss of potency. Our SAR study successfully improved the potency of the initial hit, compound **1**, from an EC_{50} value of 390 nM, all the way down to an EC_{50} value of 2 nM (compound **15**). This important achievement demonstrates that MLKL is a druggable target and provides useful chemical tools to study the function of MLKL.

Considering that certain hetero aromatic sulfonyl groups can be replaced by various nucleophiles, we speculated that the methylsulfonyl group in compound **1** may act as a leaving group for covalent binding in its interaction with MLKL.[11] To test this hypothesis, we synthesized compound **19** (Fig. 3B), a close structural analogue of compound **1**, but in which the methylsulfonyl group has no leaving ability. Compound **19** showed no potency in a necroptosis assay (Fig. S3, ESI†), indicating that covalent binding appears to be crucial for the potency of these inhibitors. We further confirmed the irreversible covalent binding behavior of compounds **12** and **15** by comparing their potency in wash/no-wash cell assays (Fig. S4, ESI†). For both compounds, the EC_{50} values recorded for the washed samples were comparable with those of the non-washed samples, suggesting that these compounds are covalent inhibitors.

Similar to compound **1**, compounds **12** and **14–16** (10 μM) did not inhibit the kinase activities of RIP1 or RIP3 in *in vitro* assays (Fig. S5, ESI†). To determine whether the direct target of this series of compounds is MLKL, we performed activity based protein profiling (ABPP; Fig. 4A). Compound **12**, an affinity probe, was incubated with MLKL-flag-HT-29 cell lysates for 2 hours, followed by a click reaction to conjugate the probe to a biotin-tag. The biotin-labeled compound–protein complexes were pulled down and analysed *via* SDS-PAGE. We observed that compound **12** could indeed covalently bind to MLKL in cell lysates and observed that compound **15** efficiently outcompeted **12** in binding to MLKL (Fig. 4B).

The BTC-ABPP method, which was developed recently in our lab, greatly facilitates the identification of probe-modified sites of target proteins in living cells (Fig. 4A).[12] Here, we used BTC-ABPP with HT-29 cells to identify the binding sites of compound **12** and MLKL. The b/y ion spectra from MS/MS analysis (Fig. 4C) revealed that the covalent binding site of compound **12** was Cys-86 in the SNICR peptide of human MLKL; this is the same residue proposed to be the site of NSA modification.[4] To further verify the relationship between probe binding at Cys-86 and the function of compounds **12** and **15** in necroptosis, MLKL-knockout RIP3-HeLa cells were transfected with wild-type or the C86S (Cysteine 86 is mutated to Serine) mutated form of MLKL. TSZ stimulation of both types of cells

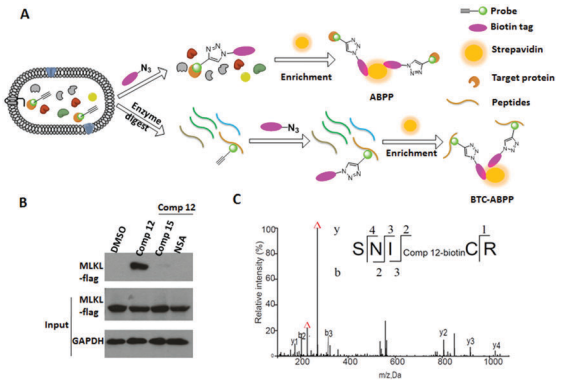

Fig. 4 Compound **12** covalently binds MLKL at Cys-86. (A) Schema of the general procedure for ABPP and BTC-ABPP. (B) Compound **12** covalently binds MLKL: HT-29 cells were incubated with compound **12** (1 μM) or DMSO for 2 h. For the binding competition experiment samples, cells were pre-incubated with 5 μM NSA or 100 nM compound **15** for 2 h; 1 μM compound **12** was then added and incubated for an additional 2 h. The click reaction (Biotin-C_2H_4-N_3 10 μM, TBTA 10 μM, $CuSO_4$ 50 μM, Sodium ascorbate 50 μM) was carried out with cell lysates for 2 h. The biotin-modified proteins were enriched and analysed by western blotting using antibodies against flag and GAPDH. (C) The b/y ion spectra from MS/MS analysis of the compound **12**-modified SNICR peptide establish that compound **12** covalently modifies Cys-86 of the SNICR peptide of MLKL. Red triangles indicate characteristic molecular ion peaks of **12**-biotin. Prior to performing BTC-ABPP, HT-29 cells were incubated with compound **12** (1 μM) for 2 h.

resulted in necroptosis, indicating that the C86S mutated form of MLKL functioned normally in transducing the necroptosis signal. Cells transfected with wild-type MLKL, but not cells transfected with C86S-MLKL, were protected from necroptosis by compounds **12** and **15**, further confirming that compounds **12** and **15** inhibit MLKL by directly binding to Cys-86 (Fig. S6, ESI†). Cys-86 in human MLKL structurally corresponds to a tryptophan residue in mouse and rat MLKL. Helix H4 at the N-terminal domain of the human MLKL structure, which contains Cys-86, is not present in mouse MLKL.[13] Given this, we speculated that compounds **12** and **15** may show poor inhibition against the function of mouse or rat MLKL in necroptosis. We performed necroptosis assays in mouse MEF and L929 cell lines and in the rat L6 cell line (Fig. S7, ESI†), and found that neither compound **12** nor compound **15** showed inhibition activity, even at concentrations higher than 50-fold excesses of their previously determined EC_{50} values. These results establish that Cys-86 of the target MLKL is required for the covalent binding and potency of this series of MLKL inhibitors.

Previous studies showed that MLKL forms homo-oligomers when it is phosphorylated by RIP3. This is a crucial step in the translocation of MLKL from the cytoplasm to the cell membrane, where it mediates ion influx and/or causes the disruption of cell structures.[5] To evaluate the mechanism of this series of compounds on MLKL, we detected the status (state of oligomerization and phosphorylation) of MLKL under TSZ stimulation in the presence of compound **12** or **15**. We first showed that compounds **12** and **15** can both block the formation of MLKL homo-oligomers (Fig. 5A). Next, we evaluated the effects of MLKL inhibitors on the

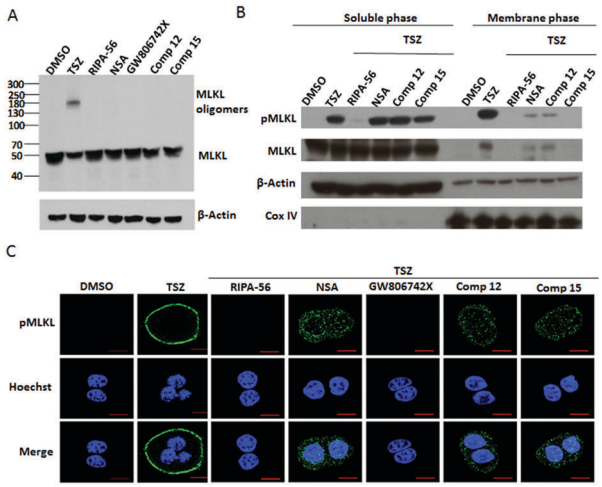

Fig. 5 Compounds **12** and **15** block the oligomerization and translocation of MLKL from the cytoplasm to the cell membrane. (A) The effects of different compounds on the oligomerization of MLKL. TSZ-treated HT-29 cells were incubated with 200 nM RIPA-56, 1 μM NSA, 1 μM GW806742X, 1 μM compound **12**, or 100 nM compound **15** for 8 h. The samples were analysed by western blotting. (B) Compounds **12** or **15** block the translocation of MLKL from the cytoplasm to the cell membrane. TSZ-treated HT-29 cells were incubated with 200 nM RIPA-56, 1 μM NSA, 1 μM compound **12**, or 100 nM compound **15** for 8 h. The cell lysates was separated to the soluble and membrane phase. The samples were analysed by western blotting with MLKL and pMLKL antibodies. β-Actin and Cox4 were used as controls for the soluble and membrane phases, respectively. (C) The effects of different compounds on the cellular localization of pMLKL. HT-29 cells were treated as indicated for 8 h. The cellular localization of pMLKL (green) was monitored by immunofluorescence as described in the ESI† (scale bars, 10 μm).

translocation of MLKL from the cytoplasm to the cell membrane. HT-29 cells were treated with TSZ in the presence of RIPA-56, NSA, compound **12**, or compound **15** for 6 h. The proteins from cell lysates were separated and the soluble phase and membrane phase were analyzed separately with anti-MLKL and anti-pMLKL antibodies (Fig. 5B). As expected, compounds **12** and **15** did not disrupt the phosphorylation of MLKL, but did decrease the level of MLKL in the membrane phase, demonstrating that these MLKL inhibitors block the translocation of MLKL to the cell membrane, thereby protecting cells from necroptosis. We also performed immunofluorescence staining in HT-29 cells using a monoclonal anti-pMLKL antibody. After TSZ stimulation, large, bright-green fluorescent dots (pMLKL) were present in the plasma membrane (Fig. 5C). RIPA-56 and GW806742X blocked the phosphorylation of MLKL completely, and no pMLKL dots were observed in cells treated with these compounds. In contrast, small pMLKL dots were dispersed in the cytoplasm of cells treated with the MLKL inhibitors NSA and compounds **12** and **15**, indicating that, NSA and compounds **12** and **15** share similar modes of action and block the translocation of MLKL to the cell membrane. These results are consistent with earlier studies.[5]

In summary, we used phenotypic screening to identify a novel MLKL inhibitor and subsequently conducted a rational SAR study that led to the discovery of the most potent MLKL inhibitors ever reported; the EC_{50} of compound **15** reached levels as low as 2 nM (see Fig. S8 for the potencies of different MLKL inhibitors in the same necroptosis assay, ESI†). We used a compound **12** affinity probe to demonstrate that these compounds act as covalent inhibitors of MLKL. Compounds **12** and **15** were found to inhibit the oligomerization and translocation of MLKL to the cell membrane. The discovery of the novel and potent MLKL inhibitors reported here will almost certainly be of benefit in exploring the biological function of MLKL, including its role in necroptosis-related disease pathogenesis.

This work was supported by the National Major Scientific and Technological Special Project for "Significant New Drugs Development" during the Twelfth Five-year Plan Period 2013ZX0950910 from the Chinese Ministry of Science and Technology.

Notes and references

1 (*a*) L. Sun and X. Wang, *Trends Biochem. Sci.*, 2014, **39**, 587–593; (*b*) M. Pasparakis and P. Vandenabeele, *Nature*, 2015, **517**, 311–320.
2 N. Holler, R. Zaru, O. Micheau, M. Thome, A. Attinger, S. Valitutti, J.-L. Bodmer, P. Schneider, B. Seed and J. Tschopp, *Nat. Immunol.*, 2000, **1**, 489–495.
3 (*a*) S. He, L. Wang, L. Miao, T. Wang, F. Du, L. Zhao and X. Wang, *Cell*, 2009, **137**, 1100–1111; (*b*) D.-W. Zhang, J. Shao, J. Lin, N. Zhang, B.-J. Lu, S.-C. Lin, M.-Q. Dong and J. Han, *Science*, 2009, **325**, 332–336.
4 L. Sun, H. Wang, Z. Wang, S. He, S. Chen, D. Liao, L. Wang, J. Yan, W. Liu and X. Lei, *Cell*, 2012, **148**, 213–227.
5 (*a*) H. Wang, L. Sun, L. Su, J. Rizo, L. Liu, L.-F. Wang, F.-S. Wang and X. Wang, *Mol. Cell*, 2014, **54**, 133–146; (*b*) Z. Cai, S. Jitkaew, J. Zhao, H.-C. Chiang, S. Choksi, J. Liu, Y. Ward, L.-g. Wu and Z.-G. Liu, *Nat. Cell Biol.*, 2014, **16**, 55–65.
6 (*a*) J. Wu, Z. Huang, J. Ren, Z. Zhang, P. He, Y. Li, J. Ma, W. Chen, Y. Zhang and X. Zhou, *Cell Res.*, 2013, **23**, 994–1006; (*b*) D. Ofengeim, Y. Ito, A. Najafov, Y. Zhang, B. Shan, J. P. DeWitt, J. Ye, X. Zhang, A. Chang and H. Vakifahmetoglu-Norberg, *Cell Rep.*, 2015, **10**, 1836–1849; (*c*) M. Pierdomenico, A. Negroni, L. Stronati, R. Vitali, E. Prete, J. Bertin, P. J. Gough, M. Aloi and S. Cucchiara, *Am. J. Gastroenterol.*, 2014, **109**, 279–287.
7 J. M. Hildebrand, M. C. Tanzer, I. S. Lucet, S. N. Young, S. K. Spall, P. Sharma, C. Pierotti, J.-M. Garnier, R. C. Dobson and A. I. Webb, *Proc. Natl. Acad. Sci. U. S. A.*, 2014, **111**, 15072–15077.
8 D. Liao, L. Sun, W. Liu, S. He, X. Wang and X. Lei, *MedChemComm*, 2014, **5**, 333–337.
9 D. M. Sammond, K. E. Nailor, J. M. Veal, R. T. Nolte, L. Wang, V. B. Knick, S. K. Rudolph, A. T. Truesdale, E. N. Nartey and J. A. Stafford, *Bioorg. Med. Chem. Lett.*, 2005, **15**, 3519–3523.
10 Y. Ren, Y. Su, L. Sun, S. He, L. Meng, D. Liao, X. Liu, Y. Ma, C. Liu, S. Li, H. Ruan, X. Lei, X. Wang and Z. Zhang, *J. Med. Chem.*, 2017, **60**, 972–986.
11 P. Lan, F. A. Romero, T. S. Malcolm, B. D. Stevens, D. Wodka and G. M. Makara, *Tetrahedron Lett.*, 2008, **49**, 1910–1914.
12 H. Sun, Y. Ren, W. Hou, L. Li, F. Zeng, S. Li, Y. Ma, X. Liu, S. Chen and Z. Zhang, *Chem. Commun.*, 2016, **52**, 10225–10228.
13 L. Su, B. Quade, H. Wang, L. Sun, X. Wang and J. Rizo, *Structure*, 2014, **22**, 1489–1500.

